do not induce inflammatory and oxidative stress responses after pharyngeal aspiration in mice [58]. Consistent with these results, clearance of SW-CNTs from the lungs is decreased in MPO-deficient mice after pharyngeal aspiration, and the inflammatory responses in MPO-deficient mice are much more robust compared with those in wild-type mice [59].

An alternative mechanism for the degradation of CNTs in vivo has been suggested because neutrophils live for only a short time in the body. Kagan et al. have shown that superoxide/nitric oxide → peroxynitrite-driven oxidative pathways of activated macrophages are involved in the "digestion" of SW-CNTs and clearance of nanoparticles from the lungs [60].

Collectively, these studies suggest new ways to control the biopersistence of CNTs through genetic or pharmacological manipulations.

11 Conclusion

A range of toxicological studies have been conducted using various functionalized nanoparticles, cell lines, incubation conditions, agglomerations and aggregations, doses, and observation endpoints. It is therefore difficult to obtain systematic information about the interrelationships among the physicochemical properties and biological effects of nanoparticles. More rational methodologies must be developed to allow interpretation of the overarching information contained in the experimental data. Furthermore, since there is usually a difference between in vitro and in vivo results, an in vitro experimental system that mimics conditions in vivo is needed. Information collected by using this system would be useful for gaining a better understanding of the potential health risks of nanoparticles to humans. A detailed understanding of the toxicological properties of nanoparticles and balanced evaluations of risk–benefit ratios will be required before we can begin to develop safe and efficacious nanomedicines for routine clinical use.

References

1. He C, Hu Y, Yin L, Tang C, Yin C (2010) Effects of particle size and surface charge on cellular uptake and biodistribution of polymeric nanoparticles. Biomaterials 31:3657–3666
2. Yamashita K, Yoshioka Y, Higashisaka K, Mimura K, Morishita Y, Nozaki M, Yoshida T, Ogura T, Nabeshi H, Nagano K, Abe Y, Kamada H, Monobe Y, Imazawa T, Aoshima H, Shishido K, Kawai Y, Mayumi T, Tsunoda S, Itoh N, Yoshikawa T, Yanagihara I, Saito S, Tsutsumi Y (2011) Silica and titanium dioxide nanoparticles cause pregnancy complications in mice. Nat Nanotechnol 6:321–328
3. Qiu Y, Liu Y, Wang L, Xu L, Bai R, Ji Y, Wu X, Zhao Y, Li Y, Chen C (2010) Surface chemistry and aspect ratio mediated cellular uptake of Au nanorods. Biomaterials 31:7606–7619
4. Huang K, Ma H, Liu J, Huo S, Kumar A, Wei T, Zhang X, Jin S, Gan Y, Wang PC, He S, Zhang X, Liang XJ (2012) Size-dependent localization and penetration of ultrasmall gold

nanoparticles in cancer cells, multicellular spheroids, and tumors in vivo. ACS Nano 6:4483–4493

5. Takagi A, Hirose A, Nishimura T, Fukumori N, Ogata A, Ohashi N, Kitajima S, Kanno J (2008) Induction of mesothelioma in p53+/− mouse by intraperitoneal application of multi-wall carbon nanotube. J Toxicol Sci 33: 105–116
6. Poland CA, Duffin R, Kinloch I, Maynard A, Wallace WA, Seaton A, Stone V, Brown S, Macnee W, Donaldson K (2008) Carbon nanotubes introduced into the abdominal cavity of mice show asbestos-like pathogenicity in a pilot study. Nat Nanotechnol 3:423–428
7. Nagai H, Okazaki Y, Chew SH, Misawa N, Yamashita Y, Akatsuka S, Ishihara T, Yamashita K, Yoshikawa Y, Yasui H, Jiang L, Ohara H, Takahashi T, Ichihara G, Kostarelos K, Miyata Y, Shinohara H, Toyokuni S (2011) Diameter and rigidity of multiwalled carbon nanotubes are critical factors in mesothelial injury and carcinogenesis. Proc Natl Acad Sci U S A 108:E1330–E1338
8. Jiang W, Kim BY, Rutka JT, Chan WC (2008) Nanoparticle-mediated cellular response is size-dependent. Nat Nanotechnol 3:145–150
9. Albanese A, Chan WC (2011) Effect of gold nanoparticle aggregation on cell uptake and toxicity. ACS Nano 5:5478–5489
10. Jiang X, Dausend J, Hafner M, Musyanovych A, Rocker C, Landfester K, Mailander V, Nienhaus GU (2010) Specific effects of surface amines on polystyrene nanoparticles in their interactions with mesenchymal stem cells. Biomacromolecules 11:748–753
11. Li R, Wang X, Ji Z, Sun B, Zhang H, Chang CH, Lin S, Meng H, Liao YP, Wang M, Li Z, Hwang AA, Song TB, Xu R, Yang Y, Zink JI, Nel AE, Xia T (2013) Surface charge and cellular processing of covalently functionalized multiwall carbon nanotubes determine pulmonary toxicity. ACS Nano 7:2352–2368
12. Chithrani BD, Ghazani AA, Chan WC (2006) Determining the size and shape dependence of gold nanoparticle uptake into mammalian cells. Nano Lett 6:662–668
13. Chithrani BD, Chan WC (2007) Elucidating the mechanism of cellular uptake and removal of protein-coated gold nanoparticles of different sizes and shapes. Nano Lett 7:1542–1550
14. Agarwal R, Singh V, Jurney P, Shi L, Sreenivasan SV, Roy K (2013) Mammalian cells preferentially internalize hydrogel nanodiscs over nanorods and use shape-specific uptake mechanisms. Proc Natl Acad Sci U S A 110: 17247–17252
15. Mukai Y, Yoshioka Y, Tsutsumi Y (2005) Phage display and PEGylation of therapeutic proteins. Comb Chem High Throughput Screen 8:145–152
16. von Maltzahn G, Park JH, Agrawal A, Bandaru NK, Das SK, Sailor MJ, Bhatia SN (2009) Computationally guided photothermal tumor therapy using long-circulating gold nanorod antennas. Cancer Res 69:3892–3900
17. Lipka J, Semmler-Behnke M, Sperling RA, Wenk A, Takenaka S, Schleh C, Kissel T, Parak WJ, Kreyling WG (2010) Biodistribution of PEG-modified gold nanoparticles following intratracheal instillation and intravenous injection. Biomaterials 31:6574–6581
18. Yoshioka Y, Tsunoda S, Tsutsumi Y (2011) Development of a novel DDS for site-specific PEGylated proteins. Chem Cent J 5:25
19. Rodriguez PL, Harada T, Christian DA, Pantano DA, Tsai RK, Discher DE (2013) Minimal "Self" peptides that inhibit phagocytic clearance and enhance delivery of nanoparticles. Science 339:971–975
20. Ou Z, Wu B, Xing D, Zhou F, Wang H, Tang Y (2009) Functional single-walled carbon nanotubes based on an integrin alpha v beta 3 monoclonal antibody for highly efficient cancer cell targeting. Nanotechnology 20:105102
21. Wang CH, Chiou SH, Chou CP, Chen YC, Huang YJ, Peng CA (2011) Photothermolysis of glioblastoma stem-like cells targeted by carbon nanotubes conjugated with CD133 monoclonal antibody. Nanomedicine 7:69–79
22. Ruggiero A, Villa CH, Bander E, Rey DA, Bergkvist M, Batt CA, Manova-Todorova K, Deen WM, Scheinberg DA, McDevitt MR (2010) Paradoxical glomerular filtration of carbon nanotubes. Proc Natl Acad Sci U S A 107:12369–12374
23. Tenzer S, Docter D, Kuharev J, Musyanovych A, Fetz V, Hecht R, Schlenk F, Fischer D, Kiouptsi K, Reinhardt C, Landfester K, Schild H, Maskos M, Knauer SK, Stauber RH (2013) Rapid formation of plasma protein corona critically affects nanoparticle pathophysiology. Nat Nanotechnol 8:772–781
24. Tenzer S, Docter D, Rosfa S, Wlodarski A, Kuharev J, Rekik A, Knauer SK, Bantz C, Nawroth T, Bier C, Sirirattanapan J, Mann W, Treuel L, Zellner R, Maskos M, Schild H, Stauber RH (2011) Nanoparticle size is a critical physicochemical determinant of the human blood plasma corona: a comprehensive quantitative proteomic analysis. ACS Nano 5: 7155–7167
25. Lesniak A, Fenaroli F, Monopoli MP, Aberg C, Dawson KA, Salvati A (2012) Effects of the

presence or absence of a protein corona on silica nanoparticle uptake and impact on cells. ACS Nano 6:5845–5857

26. Ge C, Du J, Zhao L, Wang L, Liu Y, Li D, Yang Y, Zhou R, Zhao Y, Chai Z, Chen C (2011) Binding of blood proteins to carbon nanotubes reduces cytotoxicity. Proc Natl Acad Sci U S A 108:16968–16973
27. Deng ZJ, Liang M, Monteiro M, Toth I, Minchin RF (2011) Nanoparticle-induced unfolding of fibrinogen promotes Mac-1 receptor activation and inflammation. Nat Nanotechnol 6:39–44
28. Schleh C, Rothen-Rutishauser B, Kreyling WG (2011) The influence of pulmonary surfactant on nanoparticulate drug delivery systems. Eur J Pharm Biopharm 77:350–352
29. Gasser M, Rothen-Rutishauser B, Krug HF, Gehr P, Nelle M, Yan B, Wick P (2010) The adsorption of biomolecules to multi-walled carbon nanotubes is influenced by both pulmonary surfactant lipids and surface chemistry. J Nanobiotechnol 8:31
30. Konduru NV, Tyurina YY, Feng W, Basova LV, Belikova NA, Bayir H, Clark K, Rubin M, Stolz D, Vallhov H, Scheynius A, Witasp E, Fadeel B, Kichambare PD, Star A, Kisin ER, Murray AR, Shvedova AA, Kagan VE (2009) Phosphatidylserine targets single-walled carbon nanotubes to professional phagocytes in vitro and in vivo. PLoS One 4:e4398
31. Kapralov AA, Feng WH, Amoscato AA, Yanamala N, Balasubramanian K, Winnica DE, Kisin ER, Kotchey GP, Gou P, Sparvero LJ, Ray P, Mallampalli RK, Klein-Seetharaman J, Fadeel B, Star A, Shvedova AA, Kagan VE (2012) Adsorption of surfactant lipids by single-walled carbon nanotubes in mouse lung upon pharyngeal aspiration. ACS Nano 6: 4147–4156
32. Peng Q, Zhang S, Yang Q, Zhang T, Wei XQ, Jiang L, Zhang CL, Chen QM, Zhang ZR, Lin YF (2013) Preformed albumin corona, a protective coating for nanoparticles based drug delivery system. Biomaterials 34:8521–8530
33. Wang Z, Liu S, Ma J, Qu G, Wang X, Yu S, He J, Liu J, Xia T, Jiang GB (2013) Silver nanoparticles induced RNA polymerase-silver binding and RNA transcription inhibition in erythroid progenitor cells. ACS Nano 7:4171–4186
34. Falaschetti CA, Paunesku T, Kurepa J, Nanavati D, Chou SS, De M, Song M, Jang JT, Wu A, Dravid VP, Cheon J, Smalle J, Woloschak GE (2013) Negatively charged metal oxide nanoparticles interact with the 20S proteasome and differentially modulate its biologic functional effects. ACS Nano 7:7759–7772
35. Vonarbourg A, Passirani C, Saulnier P, Simard P, Leroux JC, Benoit JP (2006) Evaluation of pegylated lipid nanocapsules versus complement system activation and macrophage uptake. J Biomed Mater Res A 78:620–628
36. Vonarbourg A, Passirani C, Saulnier P, Benoit JP (2006) Parameters influencing the stealthiness of colloidal drug delivery systems. Biomaterials 27:4356–4373
37. Reddy ST, van der Vlies AJ, Simeoni E, Angeli V, Randolph GJ, O'Neil CP, Lee LK, Swartz MA, Hubbell JA (2007) Exploiting lymphatic transport and complement activation in nanoparticle vaccines. Nat Biotechnol 25: 1159–1164
38. Thomas SN, van der Vlies AJ, O'Neil CP, Reddy ST, Yu SS, Giorgio TD, Swartz MA, Hubbell JA (2011) Engineering complement activation on polypropylene sulfide vaccine nanoparticles. Biomaterials 32:2194–2203
39. Bihari P, Holzer M, Praetner M, Fent J, Lerchenberger M, Reichel CA, Rehberg M, Lakatos S, Krombach F (2010) Single-walled carbon nanotubes activate platelets and accelerate thrombus formation in the microcirculation. Toxicology 269:148–154
40. Meng J, Cheng X, Liu J, Zhang W, Li X, Kong H, Xu H (2012) Effects of long and short carboxylated or aminated multiwalled carbon nanotubes on blood coagulation. PLoS One 7:e38995
41. Nemmar A, Melghit K, Ali BH (2008) The acute proinflammatory and prothrombotic effects of pulmonary exposure to rutile TiO2 nanorods in rats. Exp Biol Med (Maywood) 233:610–619
42. Burke AR, Singh RN, Carroll DL, Owen JD, Kock ND, D'Agostino R Jr, Torti FM, Torti SV (2011) Determinants of the thrombogenic potential of multiwalled carbon nanotubes. Biomaterials 32:5970–5978
43. Nabeshi H, Yoshikawa T, Matsuyama K, Nakazato Y, Arimori A, Isobe M, Tochigi S, Kondoh S, Hirai T, Akase T, Yamashita T, Yamashita K, Yoshida T, Nagano K, Abe Y, Yoshioka Y, Kamada H, Imazawa T, Itoh N, Kondoh M, Yagi K, Mayumi T, Tsunoda S, Tsutsumi Y (2012) Amorphous nanosilicas induce consumptive coagulopathy after systemic exposure. Nanotechnology 23:045101
44. Yoshida T, Yoshioka Y, Tochigi S, Hirai T, Uji M, Ichihashi K, Nagano K, Abe Y, Kamada H, Tsunoda S, Nabeshi H, Higashisaka K, Yoshikawa T, Tsutsumi Y (2013) Intranasal exposure to amorphous nanosilica particles could activate intrinsic coagulation cascade and platelets in mice. Part Fibre Toxicol 10:41

45. Morishige T, Yoshioka Y, Inakura H, Tanabe A, Narimatsu S, Yao X, Monobe Y, Imazawa T, Tsunoda S, Tsutsumi Y, Mukai Y, Okada N, Nakagawa S (2012) Suppression of nanosilica particle-induced inflammation by surface modification of the particles. Arch Toxicol 86:1297–1307
46. Schwartz J (1994) Air pollution and hospital admissions for the elderly in Detroit, Michigan. Am J Respir Crit Care Med 150:648–655
47. Pope CA 3rd, Burnett RT, Thun MJ, Calle EE, Krewski D, Ito K, Thurston GD (2002) Lung cancer, cardiopulmonary mortality, and long-term exposure to fine particulate air pollution. JAMA 287:1132–1141
48. Neupane B, Jerrett M, Burnett RT, Marrie T, Arain A, Loeb M (2010) Long-term exposure to ambient air pollution and risk of hospitalization with community-acquired pneumonia in older adults. Am J Respir Crit Care Med 181:47–53
49. Shvedova AA, Fabisiak JP, Kisin ER, Murray AR, Roberts JR, Tyurina YY, Antonini JM, Feng WH, Kommineni C, Reynolds J, Barchowsky A, Castranova V, Kagan VE (2008) Sequential exposure to carbon nanotubes and bacteria enhances pulmonary inflammation and infectivity. Am J Respir Cell Mol Biol 38: 579–590
50. Kim JS, Adamcakova-Dodd A, O'Shaughnessy PT, Grassian VH, Thorne PS (2011) Effects of copper nanoparticle exposure on host defense in a murine pulmonary infection model. Part Fibre Toxicol 8:29
51. Kodali V, Littke MH, Tilton SC, Teeguarden JG, Shi L, Frevert CW, Wang W, Pounds JG, Thrall BD (2013) Dysregulation of macrophage activation profiles by engineered nanoparticles. ACS Nano 7:6997–7010
52. Chao Y, Karmali PP, Mukthavaram R, Kesari S, Kouznetsova VL, Tsigelny IF, Simberg D (2013) Direct recognition of superparamagnetic nanocrystals by macrophage scavenger receptor SR-AI. ACS Nano 7:4289–4298
53. Tsai CY, Lu SL, Hu CW, Yeh CS, Lee GB, Lei HY (2012) Size-dependent attenuation of TLR9 signaling by gold nanoparticles in macrophages. J Immunol 188:68–76
54. Sumbayev VV, Yasinska IM, Garcia CP, Gilliland D, Lall GS, Gibbs BF, Bonsall DR, Varani L, Rossi F, Calzolai L (2013) Gold nanoparticles downregulate interleukin-1beta-induced pro-inflammatory responses. Small 9:472–477
55. Tkach AV, Shurin GV, Shurin MR, Kisin ER, Murray AR, Young SH, Star A, Fadeel B, Kagan VE, Shvedova AA (2011) Direct effects of carbon nanotubes on dendritic cells induce immune suppression upon pulmonary exposure. ACS Nano 5:5755–5762
56. Tkach AV, Yanamala N, Stanley S, Shurin MR, Shurin GV, Kisin ER, Murray AR, Pareso S, Khaliullin T, Kotchey GP, Castranova V, Mathur S, Fadeel B, Star A, Kagan VE, Shvedova AA (2013) Graphene oxide, but not fullerenes, targets immunoproteasomes and suppresses antigen presentation by dendritic cells. Small 9:1686–1690
57. Yanes RE, Tarn D, Hwang AA, Ferris DP, Sherman SP, Thomas CR, Lu J, Pyle AD, Zink JI, Tamanoi F (2013) Involvement of lysosomal exocytosis in the excretion of mesoporous silica nanoparticles and enhancement of the drug delivery effect by exocytosis inhibition. Small 9:697–704
58. Kagan VE, Konduru NV, Feng W, Allen BL, Conroy J, Volkov Y, Vlasova II, Belikova NA, Yanamala N, Kapralov A, Tyurina YY, Shi J, Kisin ER, Murray AR, Franks J, Stolz D, Gou P, Klein-Seetharaman J, Fadeel B, Star A, Shvedova AA (2010) Carbon nanotubes degraded by neutrophil myeloperoxidase induce less pulmonary inflammation. Nat Nanotechnol 5:354–359
59. Shvedova AA, Kapralov AA, Feng WH, Kisin ER, Murray AR, Mercer RR, St Croix CM, Lang MA, Watkins SC, Konduru NV, Allen BL, Conroy J, Kotchey GP, Mohamed BM, Meade AD, Volkov Y, Star A, Fadeel B, Kagan VE (2012) Impaired clearance and enhanced pulmonary inflammatory/fibrotic response to carbon nanotubes in myeloperoxidase-deficient mice. PLoS One 7:e30923
60. Kagan VE, Kapralov AA, St Croix CM, Watkins SC, Kisin ER, Kotchey GP, Balasubramanian K, Vlasova II, Yu J, Kim K, Seo W, Mallampalli RK, Star A, Shvedova AA (2014) Lung macrophages "digest" carbon nanotubes using a superoxide/peroxynitrite oxidative pathway. ACS Nano 8:5610–5621

Protein corona changes mediated by surface modification of amorphous silica nanoparticles suppress acute toxicity and activation of intrinsic coagulation cascade in mice

IOP Publishing Nanotechnology

Nanotechnology **26** (2015) 245101 (9pp) doi:10.1088/0957-4484/26/24/245101

Protein corona changes mediated by surface modification of amorphous silica nanoparticles suppress acute toxicity and activation of intrinsic coagulation cascade in mice

Tokuyuki Yoshida[1], Yasuo Yoshioka[1,2,3], Yuki Morishita[1], Michihiko Aoyama[1], Saeko Tochigi[1], Toshiro Hirai[1], Kota Tanaka[1], Kazuya Nagano[1], Haruhiko Kamada[4,5], Shin-ichi Tsunoda[4,5], Hiromi Nabeshi[6], Tomoaki Yoshikawa[1], Kazuma Higashisaka[1] and Yasuo Tsutsumi[1,5,7]

[1] Laboratory of Toxicology and Safety Science, Graduate School of Pharmaceutical Sciences, Osaka University, 1-6 Yamadaoka, Suita, Osaka 565-0871, Japan
[2] Vaccine Creation Project, BIKEN Innovative Vaccine Research Alliance Laboratories, Research Institute for Microbial Diseases, Osaka University, 3-1 Yamadaoka, Suita, Osaka 565-0871, Japan
[3] BIKEN Center for Innovative Vaccine Research and Development, The Research Foundation for Microbial Diseases of Osaka University, 3-1 Yamadaoka, Suita, Osaka 565-0871, Japan
[4] Laboratory of Biopharmaceutical Research, National Institutes of Biomedical Innovation, Health and Nutrition, 7-6-8 Saitoasagi, Ibaraki, Osaka 567-0085, Japan
[5] The Center for Advanced Medical Engineering and Informatics, Osaka University, 1-6 Yamadaoka, Suita, Osaka 565-0871, Japan.
[6] Division of Foods, National Institute of Health Sciences, 1-18-1, Kamiyoga, Setagaya-ku, Tokyo 158-8501, Japan
[7] Laboratory of Innovative Antibody Engineering and Design, Center for Drug Design Research, National Institutes of Biomedical Innovation, Health and Nutrition, 7-6-8 Saitoasagi, Ibaraki, Osaka 567-0085, Japan

E-mail: y-yoshioka@biken.osaka-u.ac.jp and ytsutsumi@phs.osaka-u.ac.jp

Received 23 January 2015, revised 7 April 2015
Accepted for publication 28 April 2015
Published 26 May 2015

Abstract

Recently, nanomaterial-mediated biological effects have been shown to be governed by the interaction of nanomaterials with some kinds of proteins in biological fluids, and the physical characteristics of the nanomaterials determine the extent and type of their interactions with proteins. Here, we examined the relationships between the surface properties of amorphous silica nanoparticles with diameters of 70 nm (nSP70), their interactions with some proteins in biological fluids, and their toxicity in mice after intravenous administration. The surface modification of nSP70 with amino groups (nSP70-N) prevented acute lethality and abnormal activation of the coagulation cascade found in the nSP70-treated group of mice. Since our previous study showed that coagulation factor XII played a role in the nSP70-mediated abnormal activation of the coagulation cascade, we examined the interaction of nSP70 and nSP70-N with coagulation factor XII. Coagulation factor XII bonded to the surface of nSP70 to a greater extent than that observed for nSP70-N, and consequently more activation of coagulation factor XII was observed for nSP70 than for nSP70-N. Collectively, our results suggest that controlling the interaction of nSP70 with blood coagulation factor XII by modifying the surface properties would help to inhibit the nSP70-mediated abnormal activation of the blood coagulation cascade.

Keywords: coagulation, nanoparticles, protein adsorption, surface modification

1. Introduction

With the recent development of nanotechnology, many nanomaterials with innovative functions have been developed. Nanomaterials have a broad range of potential applications, including foods, cosmetics, and medicine, owing to their extraordinary mechanical, electronic, and biological properties [1–3]. Since human exposure to nanomaterials will increase in the future, the development of more effective and safer forms of nanomaterials is urgently needed. Some recent studies have reported that nanomaterials may have unforeseen biological effects that their conventional-sized analogues do not possess. In our previous study, we revealed that silica nanoparticles with sizes smaller than 100 nm were more likely to cause consumptive coagulopathy [4, 5], pregnancy complications [6], and immune-modulating effects [7, 8] in mice compared to silica particles with sizes larger than 100 nm. Therefore, to improve nanomaterials' safety for future biological or biomedical applications, we need to acquire information not only about these materials' unforeseen biological effects but also about how to reduce or avoid undesirable biological effects. Nanomaterial-mediated biological effects are known to be related to the physical characteristics of nanomaterials, such as particle size and surface properties. In this regard, some groups have shown that the surface properties of nanomaterials are related to their cellular responses, such as cellular uptake or toxicity [9, 10]. Oh *et al* showed that, for a comparison among surface-modified silica–titania hollow nanoparticles with cationic, anionic, and neutral functional groups, cationic silica–titania hollow nanoparticles demonstrated the most toxic effects on mouse alveolar macrophages and the highest uptake efficiency [9]. Asati *et al* reported that cerium oxide nanoparticles with different surface charges (positive, negative, and neutral) exhibited different internalization and localization in cells, resulting in the induction of different cytotoxicity profiles [10]. In addition, we previously revealed that silica-nanoparticle-mediated pregnancy complications, inflammation, reactive oxygen species generation, or DNA damage could be reduced by surface modification of the silica nanoparticles with amino or carboxyl groups [6, 11, 12]. All of these previous findings suggest that surface modification of silica nanoparticles with amino or carboxyl groups may be effective for the creation of safer silica nanoparticles. However, it is not fully understood why the surface modification of silica nanoparticles by amino or carboxyl groups mitigates undesirable, silica-nanoparticle-mediated biological effects.

When nanomaterials enter the body, they are expected to become coated with various proteins and form a protein corona that may induce biological effects [13]. Many studies have suggested that interactions between proteins and nanomaterials play an important role in the biological effects or biodistribution of nanomaterials [14]. The extent of protein binding to nanomaterials depends on the physicality of the nanomaterials; thus, the nanomaterials' size or surface properties are very important in determining the extent of interactions between proteins and nanomaterials [13, 15]. Thus, it is possible that our previously reported reduction of undesirable, silica-nanoparticle-mediated biological effects by surface modification with amino or carboxyl groups might be attributable to the formation of a protein corona.

In our previous study, we showed that silica nanoparticles with sizes smaller than 100 nm could cause consumptive coagulopathy using intravenous administration [4], however, we did not investigate the effect of surface modification of silica nanoparticles on the silica nanoparticles-induced undesirable biological effects. Here, to reveal why the surface modification of silica nanoparticles by amino groups mitigates undesirable silica-nanoparticle-mediated biological effects, using intravenous administration, we investigated the effect of surface modification by amino groups on the silica-nanoparticle-induced acute toxicity and activation of coagulation cascade in mice. In addition, we examined whether the interactions between proteins and nanomaterials affected the activation of coagulation cascade. We concluded that controlling the interactions between proteins and nanomaterials by means of nanoparticle surface modification is a useful method to reduce nanomaterial-mediated biological effects.

2. Materials and methods

2.1. Silica particles

Amorphous silica nanoparticles (external diameter, 70 nm) with surfaces that were either unmodified or modified with amino groups were purchased from Micromod Partikeltechnologie GmbH, Rostock, Germany (designated nSP70 or nSP70-N, respectively). According to product document of silica nanoparticles in this study, the surface of nSP70 and nSP70-N are covered with silanol group. Additionally, nSP70-N is modified by amino group through the spacer. The 25 mg mL^{-1} silica nanoparticles were sonicated for 5 min and vortexed for 1 min and diluted in phosphate-buffered saline (PBS) immediately prior to use.

2.2. Animals

BALB/c mice (female, 6–8 weeks) were purchased from Japan SLC, Inc., Shizuoka, Japan. Mice were housed in a ventilated animal room maintained at 20 ± 2 °C with a 12 h light/12 h dark cycle. Mice had free access to water and alfalfa-free forage (FR-2, Funabashi Farm, Funabashi, Japan). All of the animal experimental procedures in this study were performed in accordance with the National Institute of Biomedical Innovation and Osaka University Guidelines for the Welfare of Animals.

2.3. Inductively coupled plasma-optical emission spectrometry (ICP-OES)

Ten mice were treated with nSP70, nSP70-N, or PBS (control) at a dose of 2 mg/mouse by means of intravenous injection. Two or five hours after the intravenous injection, the livers were harvested from each group of five mice. To determine the silicon content in the liver tissues, the wet samples were weighed, digested with nitric acid by heating, and then analyzed for silicon content using inductively coupled plasma-optical emission spectrometry (ICP-OES, 735-ES, Agilent Technologies, Tokyo, Japan).

2.4. Acute lethal toxicity test

The mice were treated with nSP70, nSP70-N, or PBS as control at a dose of 2 mg/mouse by means of intravenous injection, and their survival was observed for a period of 24 h.

2.5. Blood biomarker assay

The mice were treated with nSP70, nSP70-N, or PBS (control) at a dose of 2 mg/mouse by means of intravenous injection. Five hours after intravenous injection, blood samples were collected from the heart using plastic syringes (Terumo, Tokyo, Japan) containing 5 IU mL^{-1} heparin sodium. Plasma was harvested by centrifuging the blood at $1750 \times g$ for 15 min. The levels of alanine aminotransferase (ALT), aspartate aminotransferase (AST), and blood urea nitrogen (BUN) were measured using a biochemical autoanalyzer (Fuji Dri-Chem 7000, Fujifilm, Tokyo, Japan).

2.6. Coagulation tests

Five hours after the intravenous injection with nSP70 or nSP70-N at a dose of 2 mg/mouse, blood samples were collected from the heart using plastic syringes containing 1:9 (v/v) of 3.8% sodium citrate in PBS. Plasma was harvested by centrifuging the blood at $1750 \times g$ for 15 min. The activated partial thromboplastin time (APTT) was determined at 37 °C in a Clotek dry-block bath system (Hyland Division, Travenol Laboratories, Inc. Costa Mesa, CA, USA) with APTT reagents (Sysmex, Kobe, Japan).

2.7. Hematology analysis

The mice were treated with nSP70, nSP70-N, or PBS (control) at a dose of 2 mg/mouse by means of intravenous injection. Five hours after the intravenous injection, blood samples were collected from the heart using plastic syringes (Terumo) containing 0.1 mM EDTA in PBS. Whole blood samples were analyzed with a VetScan HMII Hematology System (Abaxis, Sunnyvale, CA, USA) to determine platelet counts.

2.8. In vitro silica nanoparticle clotting time

Venous blood was collected from healthy human volunteers in plastic tubes containing 1/9 volume of 3.8% sodium citrate and centrifuged at 1750 g for 10 min at 4 °C. Factor XII-deficient plasma was purchased from Hematologic Technologies, Inc. (Essex Junction). One hundred microliters of healthy human plasma or coagulation factor XII-deficient plasma and 100 μL of nSP70, nSP70-N (0.02 mg mL^{-1} in PBS) were mixed together. After 3 min incubation at 37 °C, the resulting mixture was added to 100 μL of 20 mM $CaCl_2$ in PBS, and clotting time was recorded using the Clotek dry-block bath system (Hyland Division, Travenol Laboratories, Inc., Costa Mesa, Calif., USA).

2.9. Western blotting

Fifty microliters of nSP70 or nSP70-N (25 mg mL^{-1} in water) was incubated with 250 μL healthy human plasma (BBI Solutions, Cardiff, UK) for 5–30 min followed by centrifugation ($21\,500 \times g$ for 15 min at 4 °C) and washed by 1 mL PBS to remove all unbound proteins. The silica nanoparticles obtained after centrifugation were suspended by 10% sodium dodecyl sulfate (SDS) solution (referred to herein as the sample solution). The sample solution and Laemmli Sample Buffer (Bio-rad Laboratories, Hercules, CA, USA) were mixed in 3 μL (referred to herein as the mixture solution). Then, 2-mercaptoethanol (Invitrogen, Carlsbad, CA, USA) was added to the mixture solution, and the resulting mixture was incubated for 5 min at 95 °C. Each sample was separated by means of sodium dodecyl sulfate polyacrylamide gel electrophoresis (SDS-PAGE; 10–20% e-PAGEL, ATTO), followed by electrotransfer onto a polyvinylidene difluoride membrane (Millipore, Billerica, MA, USA). The membranes were incubated with 1% bovine serum albumin (Sigma-Aldrich, St. Louis, MO, USA) in PBS—0.05% w/w Tween20 for 2 h at room temperature. After incubating with bovine serum albumin, the membranes were incubated with specific antibodies against human coagulation factor XII (mouse anti-human factor XII monoclonal antibody, 1:50000, Abcam, Cambridge, MA, USA) for 1 h at room temperature. Then, the membranes were washed with PBS—0.05% Tween20 and incubated with goat anti-mouse IgG-peroxidase antibody (1:60000, Sigma-Aldrich) used as secondary antibodies for 1 h at room temperature. For detection, the membranes were incubated with SuperSignal West Femto Maximum Sensitivity Substrate (Thermo Scientific, Rockford, IL, USA). The protein bands on the membrane were visualized with an ImageQuant LAS 4000mini biomolecular imager (GE Healthcare). Band intensity was quantified by film densitometry using ImageJ software (National Institutes of Health, Bethesda, MD, USA).

2.10. SDS-PAGE

Fifty microliters of nSP70 or nSP70-N (25 mg mL^{-1} in water) was incubated with 50 μL recombinant human coagulation factor XII (Haematologic Technologies Inc., Essex Junction, VT, USA) for 30 min and then centrifuged ($21\,500 \times g$ for 15 min at 4 °C) and washed with 1 mL PBS. The samples were suspended in 10% SDS solution (sample solution) and separated by means of SDS-PAGE (10–20% e-PAGEL, ATTO).

2.11. Statistical analysis

Differences among each group were compared by using Bonferroni's method after analysis of variance.

3. Results

3.1. Physicochemical examinations of nSP70 and nSP70-N

In this study, we focused exclusively on amorphous silica nanoparticles, which are commonly used as additives in food and cosmetics, as well as in medical diagnostics [16, 17]. We used silica nanoparticles with a diameter of 70 nm and surfaces unmodified or modified with an amino functional group (referred to herein as nSP70 and nSP70-N, respectively). In our previous study, we examined the physicochemical properties of nSP70 and nSP70-N [6]. Close examination of silica nanoparticles by transmission electron microscopy analysis revealed that all silica nanoparticles used in this study were smooth-surfaced spherical particles [6]. The particles' size, zeta potential, and other properties were determined by dynamic light scattering measurements. The mean secondary particle diameter was 65 and 72 nm for nSP70 and nSP70-N, respectively [6]. Mean particle diameter measurements acquired in PBS revealed that these silica nanoparticles remained stable and well-dissolved in solution, without aggregating. The surface charge was −53 and −29 mV for nSP70 and nSP70-N, respectively [6].

3.2. In vivo distribution of nSP70 and nSP70-N after intravenous injection in mice

To evaluate differences in biological effects incurred by the surface modification of silica nanoparticles, we need to understand the biodistribution of the modified and unmodified silica nanoparticles. Since nSP70 induces hepatotoxicity after intravenous injection in mice [4], the mice were intravenously treated with nSP70 or nSP70-N (2 mg/mouse), and the level of silica nanoparticles in the liver was measured using ICP-OES at 2 or 5 h after administration. There were no differences in the levels of silica nanoparticles found in the liver between the nSP70-treated group and the nSP70-N-treated group (figure 1). We did not detect the silica in the liver in control group (data not shown; the detection limit of our protocol was 50 $\mu g\, g^{-1}$). Furthermore, we did not detect the particles in blood samples from the nSP70- or nSP70-N-treated groups (data not shown). Therefore, the surface modification of silica nanoparticles appeared to have had no effects on the particles' translocation to the liver in our study.

3.3. Biological effects of nSP70 and nSP70-N after intravenous administration

Previously, we revealed that excessive levels of nSP70 after intravenous administration mediated a drastic decrease in the platelet count and an abnormal activation of the coagulation cascade in mice. These results suggested that the coagulation abnormality might contribute to lethal toxicity and severe

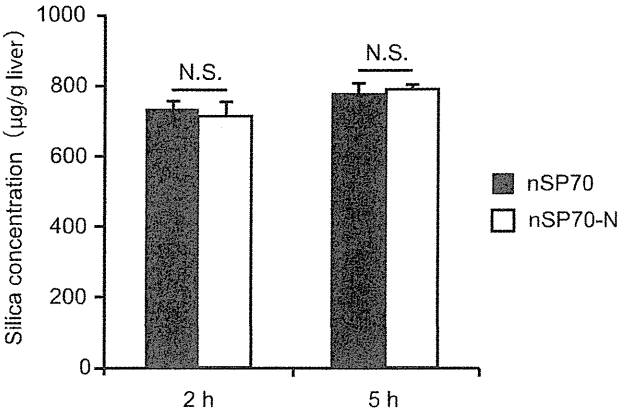

Figure 1. Biodistribution of nSP70 and nSP70-N. BALB/c mice were treated with 2 mg/mouse nSP70 or nSP70-N by intravenous injection. Two or five hours after the intravenous injection, the silicon content in the liver was analyzed by ICP-OES. N.S.: not significant. Results are expressed as mean ± S.E. ($n = 5$).

hepatotoxicity [4]. To investigate the effect of nanoparticle surface modification on acute toxicity, we observed the survival rate and measured the level of the liver damage marker ALT, AST, and kidney damage marker BUN in mice after intravenous administration of nSP70 or nSP70-N. All mice in the nSP70-treated group died within 6 h, whereas no lethal toxicity was observed in the nSP70-N-treated group even at 24 h post-administration (figure 2(a)). Five hours after the intravenous injection, although the level of ALT in the nSP70-treated group significantly increased, the level of ALT in the nSP70-N-treated group was equal to that of the control group (figure 2(b)). As with the level of ALT, the level of AST in the nSP70-treated group significantly increased, the level of AST in the nSP70-N-treated group was equal to that of the control group (figure 2(c)). The level of BUN did not change significantly for any of the groups (data not shown). In addition, to examine the effect of surface modification on the coagulation cascade, the platelet count and the APTT at 5 h after intravenous administration of nSP70 or nSP70-N were observed. Although a drastic decrease in platelet count was found in the nSP70-treated group compared to the control group, the platelet count of the nSP70-N-treated group was equal to that of the control group (figure 3(a)). Furthermore, the APTT, which is a parameter for the activation of an intrinsic coagulation pathway, of the nSP70-treated group was prolonged compared to that of the control group, whereas the APTT of the nSP70-N-treated group was significantly lower than that of the nSP70-treated group (figure 3(b)). These findings suggest that the surface modification of silica nanoparticles with amino groups could prevent silica-nanoparticle-mediated acute lethal toxicity, liver damage and abnormal activation of the coagulation cascade.

3.4. Interaction of coagulation factor XII with nSP70 and nSP70-N

Contact activation of coagulation factor XII is one of the major factors of blood coagulation. Coagulation factor XII is

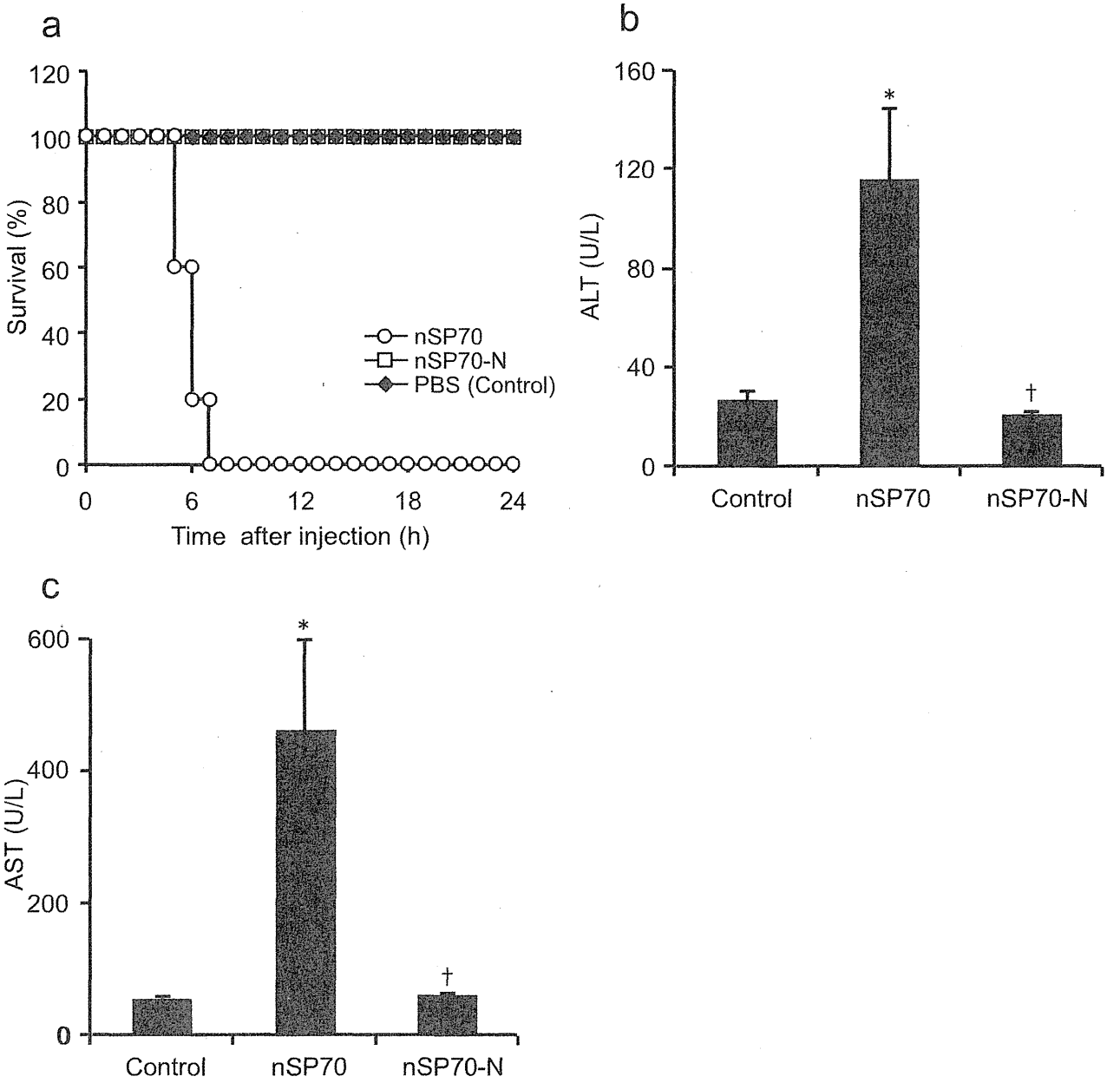

Figure 2. Acute lethal toxicity test and biochemical analysis of nSP70- and nSP70-N-treated mice. (a) Acute lethal toxicity test. BALB/c mice were treated with 2 mg/mouse nSP70, nSP70-N, and PBS (control) by intravenous injection and their survival was observed for 24 h. (b) and (c) Biochemical analysis. BALB/c mice were treated with 2 mg/mouse of nSP70, nSP70-N, and PBS (control) by intravenous injection. Five hours after the intravenous injection, blood samples were collected, and ALT(b) and AST(c) were analyzed. Results are expressed as mean ± S.E. ($n = 4$–5). The asterisk indicates a significant difference from the control group ($p < 0.01$), and the dagger indicates a significant difference from the nSP70-treated group ($p < 0.01$).

activated when it comes into contact with hydrophilic activating particles (such as fully water-wettable glass) [18]. Our previous study suggested that silica-nanoparticle-mediated activation of the coagulation cascade was related to coagulation factors, such as coagulation factor XII [4, 5]. Accordingly, prevention of the abnormal activation of the coagulation cascade by surface modification of silica nanoparticles should involve some interaction between coagulation factor XII and the nanoparticles' surface. Here, to evaluate the effect of surface modification of silica nanoparticles on the coagulation cascade, we performed *in vitro* coagulation tests using healthy human plasma or coagulation factor XII-deficient plasma. After mixing healthy human plasma or coagulation factor XII-deficient plasma with silica nanoparticles, the clotting time was recorded. The clotting time of nSP70-N-treated plasma was equal to that of the control group, whereas the clotting time of nSP70-treated plasma was significantly shorter than that of the control

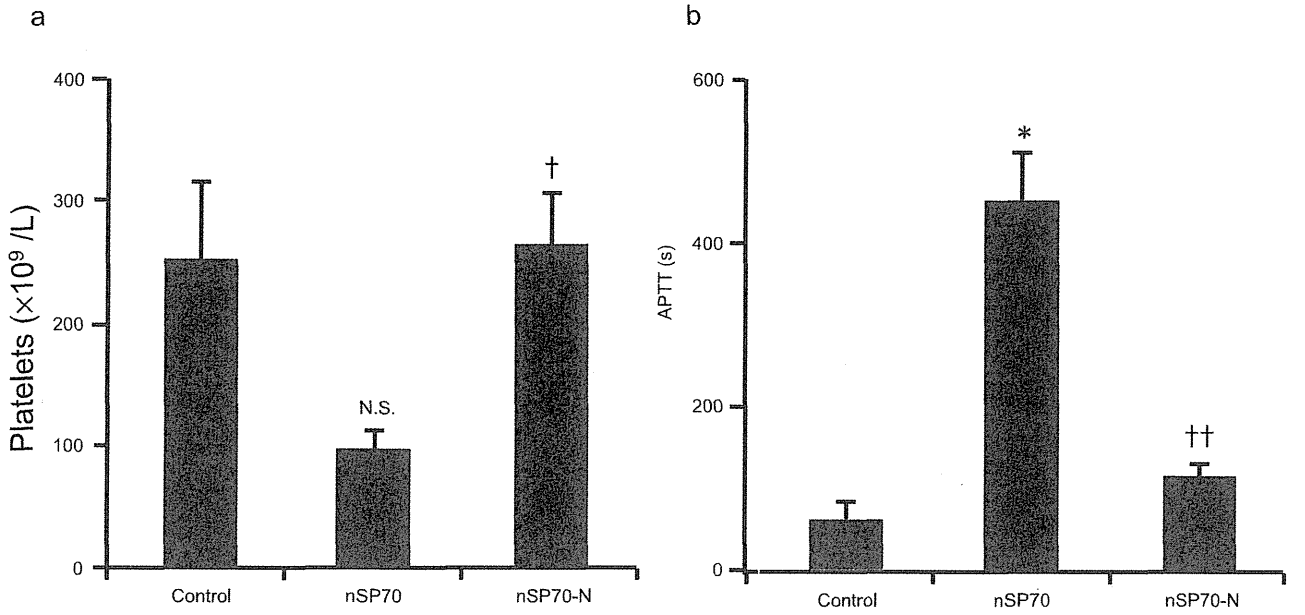

Figure 3. Platelet count analysis and coagulation tests. BALB/c mice were treated with 2 mg/mouse nSP70, nSP70-N, and PBS (control) by intravenous injection. Five hours after the intravenous injection, blood samples were collected. (a) Platelet count and (b) APTT were determined. N.S.: not significant. Results are expressed as mean ± S.E. ($n = 4$–5). The asterisk indicates a significant difference from the control group ($p < 0.01$), and the daggers indicate a significant difference from the nSP70-treated group ($^{\dagger\dagger}p < 0.01$, $^{\dagger}p < 0.05$).

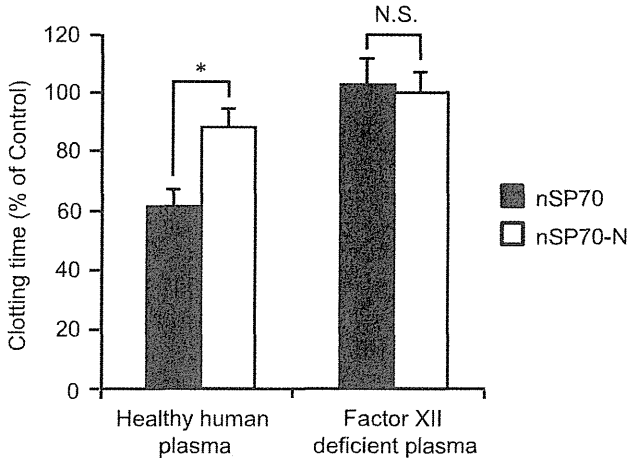

Figure 4. *In vitro* silica nanoparticle clotting time. Healthy human plasma or coagulation factor XII-deficient plasma was mixed with nSP70, nSP70-N, or PBS (control; data not shown). After 3 min incubation at 37 °C, the clotting time was evaluated. Clotting times are represented in the graphs as normalized values (i.e., the clotting time of the nSP70- or nSP70-N-treated group normalized to the clotting time of the control group.) N.S.: not significant. The asterisk indicates a significant difference between the nSP70- and nSP70-N-treated groups ($p < 0.05$).

group. In contrast, when coagulation factor XII-deficient plasma was used, the clotting times of both nSP70- and nSP70-N-treated plasma were equal to that of the control group (figure 4). These results suggest that the surface modification of silica nanoparticles reduced the particles' promotion of coagulant effects in human plasma.

To further elucidate the interaction between the surface of the silica nanoparticles and coagulation factor XII, we examined the affinity of coagulation factor XII for nSP70 or nSP70-N after mixed with healthy human plasma by means of western blot analysis (figure 5(a), *upper panel*). The incubation for 0 min means that immediate nSP70 or nSP70-N after mixed with healthy human plasma. The 80 kDa fragment showed coagulation factor XII and 40 kDa fragment were found during activation of coagulation factor XII. The band intensity of 40 kDa fragment was quantified using ImageJ software and normalized against the band of plasma only (figure 5(a), *lower panel*). The 80 kDa coagulation factor XII and a 40 kDa fragment were found in nSP70-treated groups. The relative density of 40 kDa fragment for 30 min incubation increases about 4 times than that for 0 min incubation. On the other hand, in nSP70-N-treated groups, the intensity of the 40 kDa fragment diminished with time and disappeared within 30 min. Therefore, these results suggested that it was more difficult for nSP70-N to activate coagulation factor XII compared with nSP70.

We also used SDS-PAGE to examine the affinity of coagulation factor XII for nSP70 and nSP70-N in mixtures of nSP70 or nSP70-N with recombinant human coagulation factor XII. These results showed that the intensity of the 80 kDa coagulation factor XII was more higher in nSP70-treated group than in nSP70-N-treated group. On the other hands, some small fragment between 25 and 37 kDa were found in the nSP70-N-treated group only. This suggested that nSP70-N might induce the activation of coagulation factor XII under the absence of some plasma proteins (figure 5(b)). Theses showed that some plasma proteins might have bonded to the surface of nSP70-N and thus prevented coagulation factor XII from binding to the surface of nSP70-N, thus inhibiting the activation of the coagulation cascade.

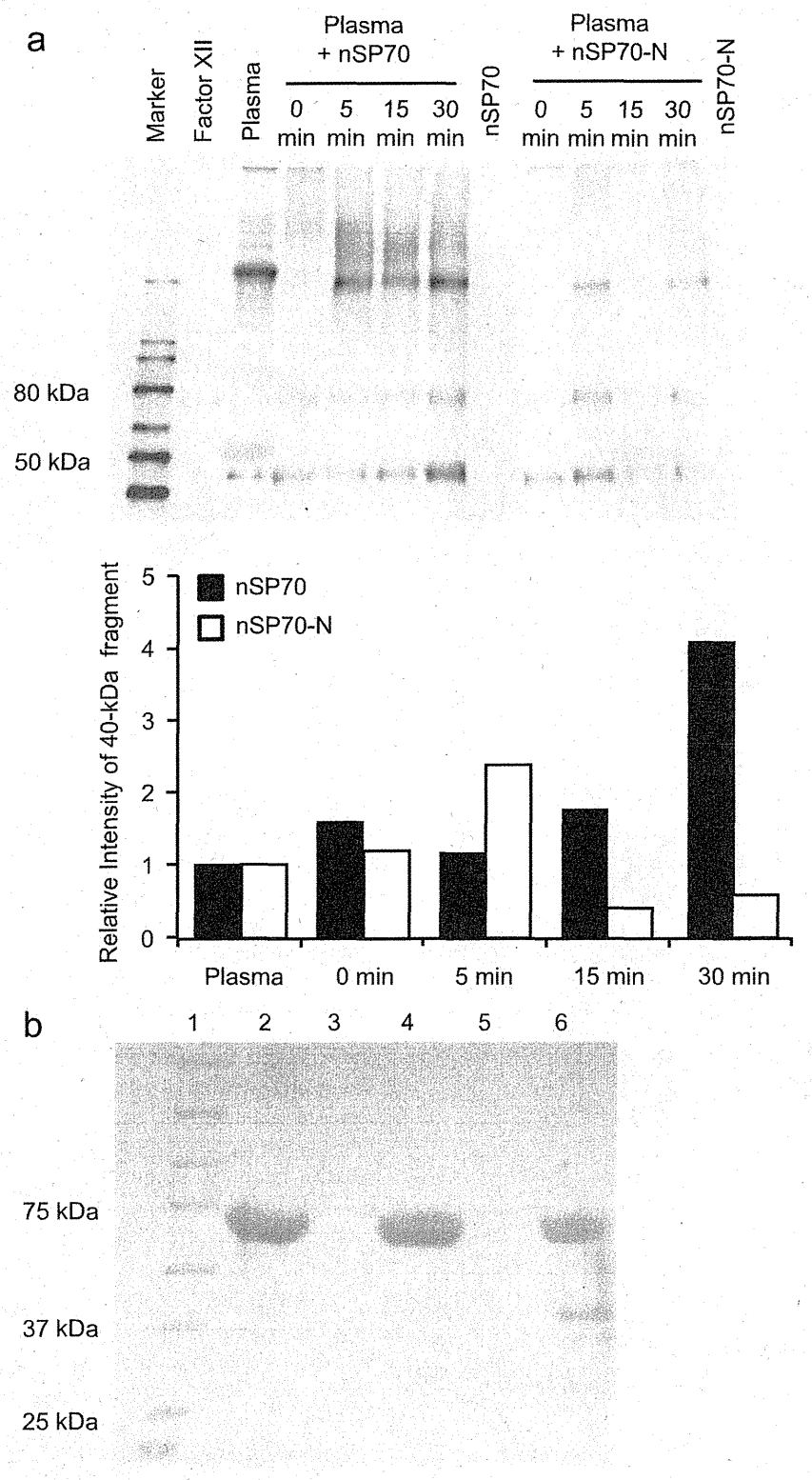

Figure 5. Interaction between silica nanoparticles and coagulation factor XII. (a) Western blot analysis of silica nanoparticles (nSP70 or nSP70-N) incubated with healthy human plasma. After incubation, the affinity between blood coagulation factor XII in the healthy human plasma and nSP70, nSP70-N was assessed by western blot (*upper panel*). The band intensity of 40 kDa fragment was quantified by film densitometry using ImageJ software and normalized against the band of plasma only (*lower panel*). (b) SDS-PAGE results for mixtures of recombinant human coagulation factor XII and nSP70 or nSP70-N. After 30 min incubation at 37 °C, the samples were separated by SDS-PAGE. Maker (Lane 1), recombinant human coagulation factor XII (Lane 2), nSP70 (Lane 3), nSP70 with recombinant human coagulation factor XII (Lane 4), nSP70-N (Lane 5), nSP70-N with recombinant human coagulation factor XII (Lane 6).

4. Discussion

Recently, the interaction of biological proteins with nanomaterials has been shown to play an important role in nanomaterial-mediated biological effects [13]. For example, a recent study suggested that the formation of a protein corona on nanomaterials reduced their undesirable cellular responses *in vitro*. Specifically, Ge *et al* suggested that the binding of blood proteins to carbon nanotubes reduced the nanotubes' cytotoxicity [19], and Hu *et al* also showed that graphene oxide-mediated cytotoxicity was attenuated by the interaction of fetal bovine serum with graphene [20]. This formation of a protein corona on nanomaterials depends on the physicality of the nanomaterials, such as their size or surface properties [15]. However, few reports have examined the relationship between surface-specific, nanomaterial-mediated biological effects and the formation of a protein corona using *in vivo* analysis.

The blood coagulation cascade can be initiated by two pathways: an extrinsic cascade pathway, which is triggered by the release of tissue factor from the site of injury, and an intrinsic cascade pathway, which is triggered by activation of a coagulant factor contacted with a negatively charged substance or accumulation of activated platelets to the collagen layer under the vascular endothelium [21]. Our previous study showed that excessive levels of silica nanoparticles induce severe hepatotoxicity, lethal toxicity, and abnormal activation of the coagulation cascade [4]. In addition, since we have shown that pretreatment of mice with the anticoagulant heparin before silica nanoparticle injection reduces the particles' lethal toxicity [4] and hepatotoxicity (data not shown), we speculated that silica-nanoparticle-mediated abnormal activation of the coagulant cascade was the main factor governing the particles' lethal toxicity. However, in the previous study, we did not examine the effect of surface modification of silica nanoparticles on biological effects using intravenous administration. Here, we investigate the effect of surface modification of silica nanoparticles by amino groups on the undesirable silica-nanoparticle-mediated biological effects. In this study, mice in nSP70-treated group died within 6 h (figure 2) and a drastic decrease in platelet count and prolongation of APTT was found in the nSP70-treated group (figure 3). This reflected the result of our previous study [4], therefore, we speculated that the cause of the nSP70s lethal toxicity is silica-nanoparticle-mediated abnormal activation of the coagulant cascade. On the other hand, we found that surface modification with amino groups could prevent the acute lethal toxicity and abnormal activation of the coagulation cascade normally observed for silica nanoparticles (figures 2 and 3). Therefore, we speculated that the surface modification of silica nanoparticles prevents silica nanoparticle induced abnormal activation of the coagulation cascade, and consequently the acute lethal toxicity was not observed in the nSP70-N-treated mice. Since there were no changes in biodistribution of particles in the liver between nSP70- and nSP70-N-treated mice (figure 1), the surface modification of silica nanoparticles plays an important role in the abnormal activation of the coagulant cascade and prevented induction of lethal toxicity without relation to the level of silica nanoparticles in the liver.

Contact activation of coagulation factor XII is one of the major events in the blood coagulation intrinsic cascade pathway [22, 23]. Our previous study showed that silica-nanoparticle-mediated abnormal activation of the coagulant cascade involved coagulation factor XII [4]. In addition, recent studies have suggested that various kinds of nanomaterials, such as silica nanoparticles and polystyrene nanoparticles, could bind coagulant factors in human plasma and form a protein corona [15, 24]. Considering these reports, we speculated that silica nanoparticles could have been transferred into the bloodstream and could have hence interacted with coagulation factor XII, which might have been the primary initiation mechanism for the observed abnormal activation of the coagulant cascade. In this study, we showed that the interaction of coagulation factor XII with nSP70 was much higher than that with nSP70-N, and that this difference in affinities for coagulation factor XII affected the clotting time of human plasma mixed with the particles (figures 4 and 5). Generally, coagulation factor XII is activated by binding to material with negative charge. Therefore, we speculated that the surface chrge is the major driving force of the interaction between silica nanoparticles and coagulation factor XII. In the future, to investigate the role of surface modification of amorphous silica nanoparticles in mice, we would need to examine the affinities of nSP70 and nSP70-N for coagulation factor XII using mouse plasma.

We concluded that the 40 kDa fragment observed in the western blots of both the nSP70- and nSP70-N-treated groups was generated during activation of coagulation factor XII, since other known activators of coagulation factor XII, such as kallikrein, also induce this 40 kDa fragment [25]. We speculated that nSP70 induced the activation of coagulation factor XII. The activated coagulation factor XII which absorbed into the surface of nSP70 was cleaved into the 40 kDa fragment (figure 5). On the other hand, we revealed that, although nSP70-N bonded to and activated recombinant coagulation factor XII, nSP70-N could not activate coagulation factor XII in plasma (figure 5). We therefore speculated that different kinds of blood proteins were absorbed on the surfaces of nSP70 and nSP70-N. Zhuo reported that the activation efficiency of hydrophobic procoagulants immersed in plasma is governed by competitive adsorption between coagulation factor XII and a host of other plasma proteins that substantially reduce the efficiency of coagulation factor XII's surface contact [26]. In addition, the formation of a protein corona has been attributed to differences in the surface charge among nanomaterials [15]. Therefore, we speculated that coagulation factor XII directly bonded to the surface of and was activated on nSP70, whereas binding to the surface of nSP70-N was more difficult owing to the presence of a protein corona on those particles' surfaces; consequently, activation of coagulation factor XII was impeded in the presence of nSP70-N compared to nSP70. Considering these observed results, we speculated that a similar response would have occurred *in vivo*. Thus, our results suggest that the interaction between silica nanoparticles and coagulant factor XII in

biological organisms is an important factor that can contribute to abnormal activation of the coagulant cascade.

In addition to the interaction between silica nanoparticles and coagulant factor XII, the interaction with blood cells, such as platelets, epithelial cells and monocytes, could impact on the biological effects. In this study, the decrease in platelet count was found in the nSP70-treated group compared to the control group, and the platelet count of the nSP70-N-treated group was equal to that of the control group (figure 3(a)). In addition, we measured the count of monocytes at five hours after the intravenous injection. Although the count of monocytes in the nSP70-treated group slightly increased, that of the nSP70-N-treated group was equal to that of the control group (date not shown). Therefore, as with plasma coagulation factors, we speculated that the difference of surface properties of silica nanoparticles would impact on the interaction with blood cells.

Recently, to support the protein corona signature of nanomaterials, some groups have used MS-based methods [27, 28]. For example, Tenzer *et al* showed that silica nanoparticles rapidly bind about 300 different proteins in plasma [27]. On the other hand, in this study, we did not show the protein corona signature of nSP70 and nSP70-N by MS-based methods. In the future, we should show the difference of formation of protein corona between nSP70 and nSP70-N, suggesting the usefulness of surface modification in forming safer nanomaterials.

5. Conclusions

We observed that the interaction of silica nanoparticles with blood proteins contributed to silica-nanoparticle-mediated, abnormal biological effects in mice. From a mechanistic standpoint, differences in the surface properties of surface-modified silica nanoparticles directly affected the particles' extent of interaction with blood proteins, such as coagulation factor XII. We expect that these findings could contribute the design of safer forms of nanomaterials.

Acknowledgments

This study was supported by Grants-in-Aid for Scientific Research from the Ministry of Education, Culture, Sports, Science and Technology of Japan (MEXT) and from the Japan Society for the Promotion of Science (JSPS); by Health Labour Sciences Research Grants from the Ministry of Health, Labour and Welfare of Japan (MHLW); by The Takeda Science Foundation; by The Research Foundation for Pharmaceutical Sciences; by The Japan Food Chemical Research Foundation; by Urakami Foundation; and by Uehara Memorial Foundation.

References

[1] Raj S, Jose S, Sumod U S and Sabitha M 2012 *J. Pharm. Bioallied Sci.* 4 186–93
[2] Wang H, Du L J, Song Z M and Chen X X 2013 *Nanomedicine* 8 2007–25
[3] Jha R K, Jha P K, Chaudhury K, Rana S V and Guha S K 2014 *Nano Rev.* 5 22762
[4] Nabeshi H *et al* 2012 *Nanotechnology* 23 045101
[5] Yoshida T *et al* 2013 *Part. Fibre Toxicol.* 10 41
[6] Yamashita K *et al* 2011 *Nat. Nanotechnology* 6 321–8
[7] Yoshida T *et al* 2011 *Nanoscale Res. Lett.* 6 195
[8] Hirai T *et al* 2012 *Part. Fibre Toxicol.* 9 3
[9] Oh W K, Kim S, Choi M, Kim C, Jeong Y S, Cho B R, Hahn J X and Jang J 2010 *ACS Nano* 4 5301–13
[10] Asati A, Santra S, Kaittanis C and Perez J M 2010 *ACS Nano* 4 5321–31
[11] Morishige T *et al* 2012 *Arch. Toxicol.* 86 1297–307
[12] Yoshida T *et al* 2012 *Biochem. Biophys. Res. Commun.* 427 748–52
[13] Monopoli M P, Aberg C, Salvati A and Dawson K A 2012 *Nat. Nanotechnology* 7 779–86
[14] Lartigue L, Wilhelm C, Servais J, Factor C, Dencausse A, Bacri J C, Luciani N and Gazeau F 2012 *ACS Nano* 6 2665–78
[15] Lundqvist M, Stigler J, Elia G, Lynch I, Cedervall T and Dawson K A 2008 *Proc. Natl Acad. Sci. USA* 105 14265–70
[16] Barik T K, Sahu B and Swain V 2008 *Parasitol. Res.* 103 253–8
[17] Knopp D, Tang D and Niessner R 2009 *Anal. Chim. Acta* 647 14–30
[18] Zhuo R, Miller R, Bussard K M, Siedlecki C A and Vogler E A 2005 *Biomaterials* 26 2965–73
[19] Ge C *et al* 2011 *Proc. Natl Acad. Sci. USA* 108 16968–73
[20] Hu W, Peng C, Lv M, Li X, Zhang Y, Chen N, Fan C and Huang Q 2011 *ACS Nano* 5 3693–700
[21] Norris L A 2003 *Best Pract. Res. Clin. Obstet. Gynaecol.* 17 369–83
[22] Colman R W 1984 *J. Clin. Invest.* 73 1249–53
[23] Colman R W and Schmaier A H 1997 *Blood* **90** 3819–43
[24] Tenzer S *et al* 2011 *ACS Nano* 5 7155–67
[25] Braat E A, Dooijewaard G and Rijken DC 1999 *Eur. J. Biochem.* 263 904–11
[26] Zhuo R, Siedlecki C A and Vogler E A 2006 *Biomaterials* 27 4325–32
[27] Tenzer S *et al* 2013 *Nat. Nanotechnology* 8 772–81
[28] Walkey C D, Olsen J B, Song F, Liu R, Guo H, Olsen D W, Cohen Y, Emili A and Chan W C 2014 *ACS Nano* 8 2439–55

Hirai et al. Particle and Fibre Toxicology (2015) 12:16
DOI 10.1186/s12989-015-0095-3

PARTICLE AND FIBRE TOXICOLOGY

RESEARCH Open Access

Cutaneous exposure to agglomerates of silica nanoparticles and allergen results in IgE-biased immune response and increased sensitivity to anaphylaxis in mice

Toshiro Hirai[1], Yasuo Yoshioka[1,2,3*], Hideki Takahashi[1,2], Ko-ichi Ichihashi[1], Asako Udaka[1], Takahide Mori[4], Nobuo Nishijima[1], Tokuyuki Yoshida[1], Kazuya Nagano[5], Haruhiko Kamada[5,6], Shin-ichi Tsunoda[5,6], Tatsuya Takagi[7,8], Ken J. Ishii[9,10], Hiromi Nabeshi[11], Tomoaki Yoshikawa[1], Kazuma Higashisaka[1,5] and Yasuo Tsutsumi[1,4,6*]

Abstract

Background: The skin is a key route of human exposure to nanomaterials, which typically occurs simultaneously with exposure to other chemical and environmental allergen. However, little is known about the hazards of nanomaterial exposure via the skin, particularly when accompanied by exposure to other substances.

Results: Repeated topical treatment of both ears and the shaved upper back of NC/Nga mice, which are models for human atopic dermatitis (AD), with a mixture of mite extract and silica nanoparticles induced AD-like skin lesions. Measurements of ear thickness and histologic analyses revealed that cutaneous exposure to silica nanoparticles did not aggravate AD-like skin lesions. Instead, concurrent cutaneous exposure to mite allergens and silica nanoparticles resulted in the low-level production of allergen-specific IgGs, including both the Th2-related IgG1 and Th1-related IgG2a subtypes, with few changes in allergen-specific IgE concentrations and in Th1 and Th2 immune responses. In addition, these changes in immune responses increased the sensitivity to anaphylaxis. Low-level IgG production was induced when the mice were exposed to allergen–silica nanoparticle agglomerates but not when the mice exposed to nanoparticles applied separately from the allergen or to well-dispersed nanoparticles.

Conclusions: Our data suggest that silica nanoparticles themselves do not directly affect the allergen-specific immune response after concurrent topical application of nanoparticles and allergen. However, when present in allergen-adsorbed agglomerates, silica nanoparticles led to a low IgG/IgE ratio, a key risk factor of human atopic allergies. We suggest that minimizing interactions between nanomaterials and allergens will increase the safety of nanomaterials applied to skin.

Keywords: Atopic dermatitis, Agglomerate, Aggregate, Anaphylaxis, Blocking antibody, IgE, IgG, Mite, Nanomaterials, Nanoparticles, Particulate matter

* Correspondence: y-yoshioka@biken.osaka-u.ac.jp; ytsutsumi@phs.osaka-u.ac.jp
[1]Laboratory of Toxicology and Safety Science, Graduate School of Pharmaceutical Sciences, Osaka University, 1-6 Yamadaoka, Suita, Osaka 565-0871, Japan
Full list of author information is available at the end of the article

Introduction

Because of their unique features and physicochemical properties [1, 2], nanomaterials are increasingly being used to add value to new and existing goods, such as cosmetics, foods, medicines, and industrial products [3–5]. However, these same novel features of nanomaterials make them hazardous under some conditions [6, 7]. To take full advantage of the potential benefits of nanomaterials, we must learn more about their hazards so that safer nanomaterials can be designed.

Numerous epidemiologic studies have prompted concerns regarding the health risks associated with exposure to nanomaterials; in particular, such studies have revealed that exposure to particulate matter (PM), including PM2.5 and Asian dust, induces many adverse effects, including facilitating the onset and severity of allergic diseases [8–11]. Because inhalational exposure to PM has been considered to be the main inducer of these adverse effects, this route has received the most attention regarding exposure to nanomaterials [12]. However, the skin is a major route of both intentional (from clothing, cosmetics, and other skin care products) and unintentional (from the environment) exposure to nanomaterials [13–15]. Furthermore, exposure to nanomaterials often occurs simultaneously with exposure to other chemical compounds and environmental allergens [16], but little is known about the hazards of cutaneous exposure to nanomaterials, particularly in combination with other substances.

In the current study, we investigated the effects of concurrent topical application of mite extract and amorphous silica nanoparticles, one of the most widely used nanomaterials, on allergic sensitization and AD in NC/Nga mice, a murine model of AD. We found that cutaneous exposure to the allergen and silica nanoparticles simultaneously did not aggravate AD-like skin lesions in the mice but resulted in low-level IgG production with little change in IgE production (IgE-biased immune response) and increased sensitivity to anaphylaxis. We suggest that an IgE-biased immune response was induced independently of the innate biologic effects of silica nanoparticles. Because a low IgG/IgE ratio is a characteristic feature of human atopic allergy, we believe that minimizing interactions between nanomaterials and allergens may improve the safety of cutaneously applied nanomaterials.

Results and discussion

Effects of co-exposure to mite allergen and silica nanoparticles in a murine model of AD

For these experiments, we used silica nanoparticles with a diameter of 30 nm (nSP30). Solutions of nSP30 were clear and colorless (Fig. 1a), and transmission electron microscopy (TEM) revealed that the particles were smooth spheres (Fig. 1b). The size distribution spectrum of nSP30 was a single peak (Fig. 1c), and the mean hydrodynamic diameter (24.1 nm, as measured by means of a dynamic light-scattering method; Fig. 1d) corresponded almost exactly to the primary particle size. These results indicate that the nSP30 particles were well dispersed in solution.

To examine the effects of co-exposure of skin to allergen and nSP30, we used an extract of the mite *Dermatophagoides pteronyssinus* (Dp) and NC/Nga mice as a model for human AD [17]. Dp is a frequent cause of many allergic conditions, including asthma and AD [18, 19]. In addition, NC/Nga mice have a genetic skin barrier defect related to low ceramide production [20]. To induce AD-like skin lesions, we repeatedly cutaneously exposed NC/Nga mice to either Dp alone or a mixture of Dp and nSP30 in an isotonic solution (phosphate buffered saline; PBS). Note that although the solutions of Dp alone and nSP30 alone were clear and colorless, the mixture of Dp + nSP30 was cloudy (Fig. 1a). TEM images suggested that mixing resulted in the formation of agglomerates (Fig. 1b), which was confirmed by the fact that the mean hydrodynamic diameter of the particles in the mixture was 1310.0 nm, which was larger than that of nSP30 alone (Fig. 1c and d). First, we confirmed that exposure to nSP30 alone did not induce the formation of topical skin lesions (Additional file 1). Comparison of the PBS and Dp-alone groups indicated that cutaneous exposure to Dp induced ear thickening, scab formation, acanthosis, inflammatory cell infiltration, and mast cell infiltration (Fig. 2a–e). The effects of cutaneous exposure to Dp + nSP30 did not differ from those of Dp alone, except that the extent of ear thickening was slightly less in the Dp + nSP30 group than in the Dp-alone group.

Total IgE levels in plasma, which are often elevated in AD and other allergic conditions [21], were measured 24 h after the final treatment. The total IgE level in the Dp-alone group was higher than that in the PBS group (Fig. 2f), and the total IgE level in the Dp + nSP30 group was slightly higher than that in the Dp-alone group (Fig. 2f). Because a Th2-mediated immune response including IgE production is unnecessary for the development of AD-like skin lesions in NC/Nga mice [22], the high total IgE level induced by cutaneous exposure to Dp + nSP30 likely did not exacerbate the Dp-induced AD-like skin lesions in NC/Nga mice.

Effect of cutaneous exposure to Dp + nSP30 on cutaneous allergic sensitization

To clarify the effect of topical Dp + nSP30 on cutaneous allergic sensitization, we evaluated the systemic immune responses 24 h after the final treatment. Although Dp-specific IgE levels were higher in both the Dp-alone group and the Dp + nSP30 group than in the PBS group, Dp-specific IgE levels did not differ significantly between the Dp-alone group and the Dp + nSP30 group (Fig. 3a).

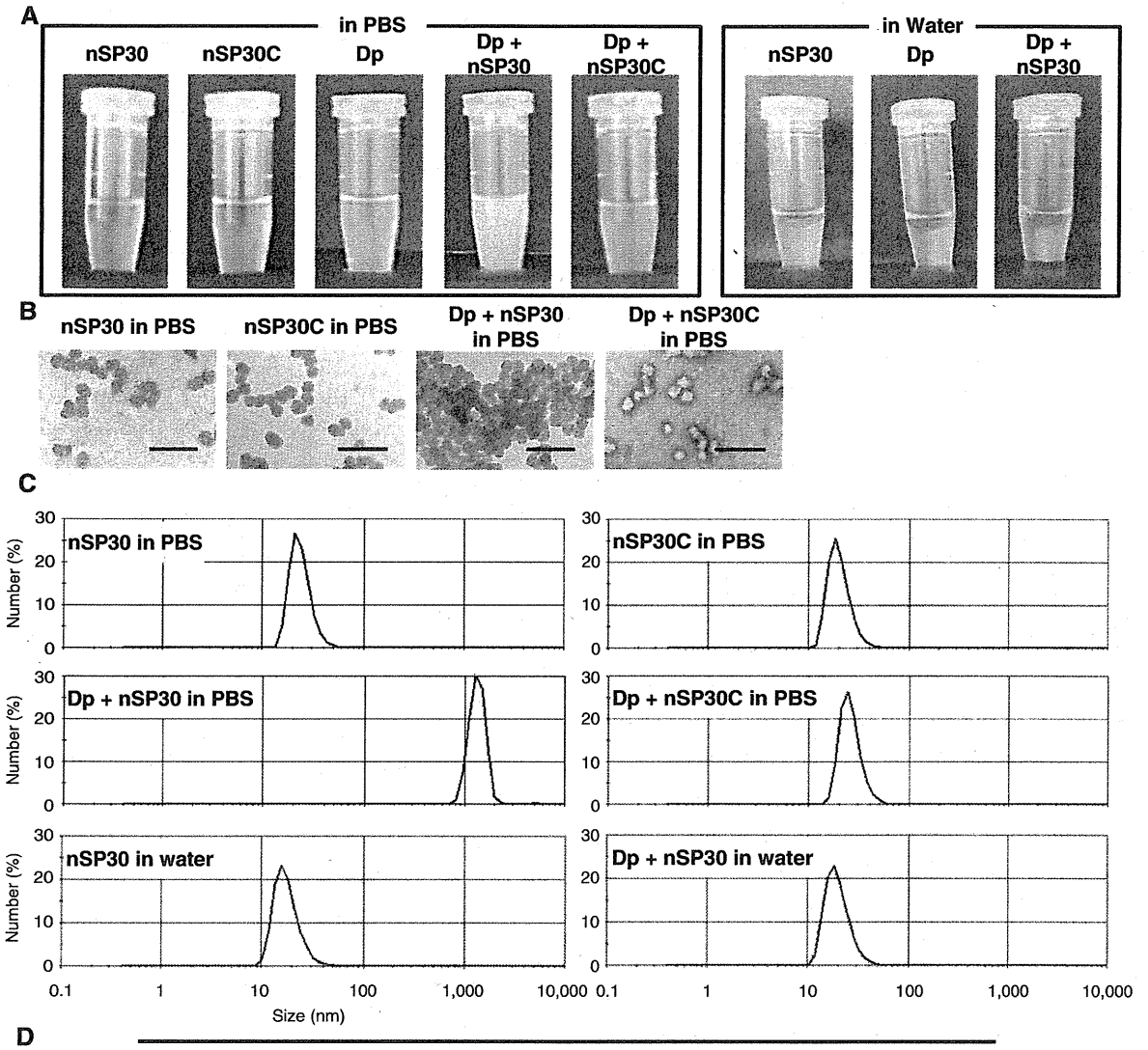

D

Sample	Vehicle	Diameter (nm)[a]	Zeta potential (mV)[b]
nSP30	PBS	24.1 ± 0.3	−24.6 ± 2.1
nSP30C	PBS	20.5 ± 0.5	−32.3 ± 0.9
Dp + nSP30	PBS	1310.0 ± 98.5	−20.2 ± 1.1
Dp + nSP30C	PBS	24.8 ± 1.1	−28.9 ± 0.0
nSP30	water	19.5 ± 1.6	Not applicable
Dp + nSP30	water	20.0 ± 0.6	Not applicable

Data are expressed as means ± SDs ($n = 3$).
[a] Peak size of histograms.
[b] pH = 7.5–7.8.

Fig. 1 Physicochemical properties of silica nanoparticles alone and combined with allergen. **a** Macroscopic and (**b**) transmission electomicrographic images of the samples used in this study (scale bar, 100 nm). **c** Particle size distributions of samples diluted in PBS or water measured by using a dynamic light scattering method. **d** Mean particle diameters and zeta potentials of samples

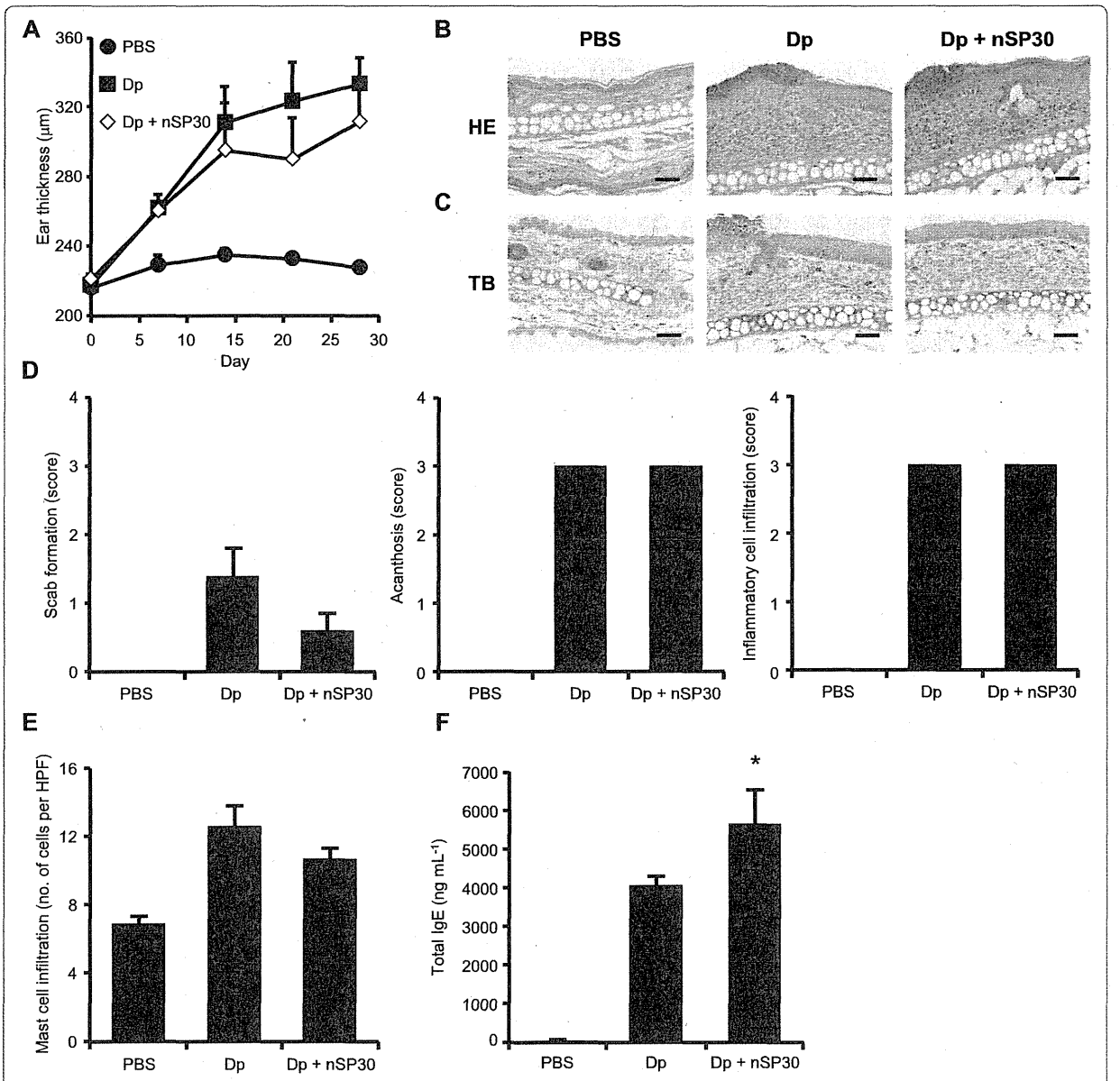

Fig. 2 Induction of AD-like skin lesions by Dp + nSP30 agglomerates in PBS. **a** Effect of topical administration of Dp alone or Dp + nSP30 in PBS on ear thickness in NC/Nga mice. b and c, Histology of ear sections stained with (**b**) hematoxylin and eosin (HE) or (**c**) toluidine blue (TB). Scale bar, 50 μm. (**d**) Scores for several symptoms characteristic of AD evaluated in HE-stained sections. **e** Mast cell infiltration evaluated in TB-stained sections as the number of mast cells per high-power (400×) field (HPF). **f** Total plasma IgE concentrations measured 24 h after the final skin painting. Data are presented as means ± SEMs ($n = 5$). *$P < 0.05$ vs. Dp-alone group

In contrast, the levels of Dp-specific total IgG and all evaluated IgG subtypes were significantly lower in the Dp + nSP30 group than in the Dp-alone group (Fig. 3b and c). In addition, we confirmed that nSP30 dose-dependently suppressed IgG production (Additional file 2). IgG subclass responses have been used to assess the type of immune response; IgG1 is known to indicate a Th2-type response, whereas IgG2a indicates a Th1 response [23]. Thus it is possible that skin exposure to Dp + nSP30 suppressed both the Th1 and the Th2 responses.

To further characterize the systemic immune responses, we enumerated the Dp-specific splenocytes secreting interferon-γ (IFN-γ) and interleukin-4 (IL-4) in each mouse by using cytokine-specific enzyme-linked immunosorbent spot (ELISPOT) assays (Fig. 3d). The numbers of Dp-specific IFN-γ- and IL-4-secreting splenocytes did not differ between the Dp-alone group and the Dp + nSP30

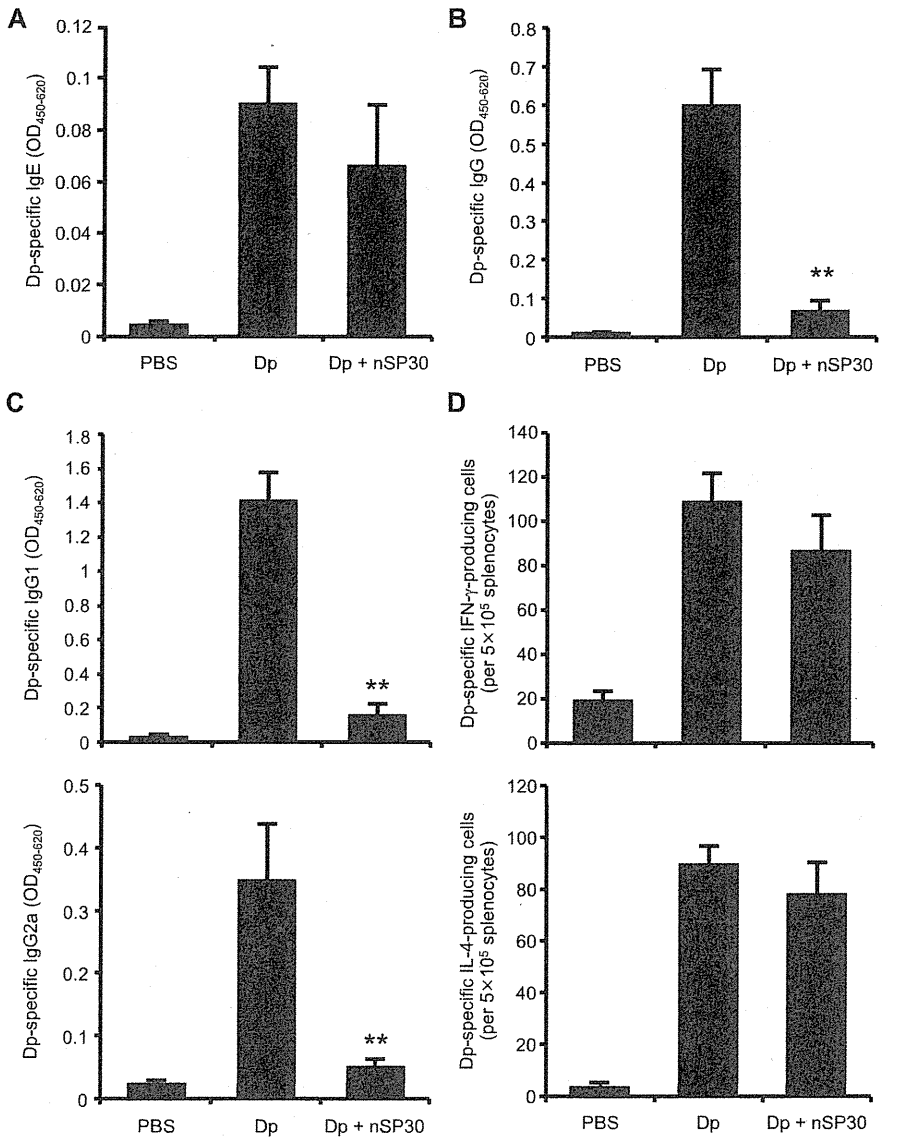

Fig. 3 Induction of systemic immune responses by Dp + nSP30 agglomerates in PBS. **a–c** Plasma levels of Dp-specific (**a**) IgE, (**b**) IgG, and (**c**) IgG1 and IgG2a as analyzed by ELISA at 24 h after final topical treatment of NC/Nga mice with Dp alone or Dp + nSP30 in PBS. (D) Numbers of Dp-specific IFN-γ- and IL-4-producing splenocytes after re-stimulation with 100 μg mL^{-1} Dp, as determined by using ELISPOT assays specific for each cytokine. Data are given as means ± SEMs ($n = 5–12$). $^{**}P < 0.01$ vs. Dp-alone group

group. In addition, although concentration of IL-21 in the supernatants of splenocytes was significantly lower in the Dp + nSP30 group than in the Dp-alone group, none of the other measured cytokines (IL-5, 10, 13, and 17) differed between these groups (Additional file 3). Therefore, nSP30 might have affected IgG production without altering systemic Th1 and Th2 immune responses. Because IL-21 is a critical factor in IgG production [24, 25], additional study of IL-21 likely would help to clarify the mechanism underlying the reductions in both the IgG1 and IgG2a subtypes.

Recently, the skin was revealed to be the key initial site of allergic sensitization not only for allergic eczema but also for other atopic allergies, including allergic rhinitis, asthma, and food allergies [26–28]. Therefore, skin might play a special role in allergic sensitization. To this end, we assessed the effects of exposure to Dp + nSP30 by various other exposure routes on the IgG response (Additional file 4). Consistent with our previously reported results [29], nSP30-mediated IgG suppression was not observed after intranasal, oral, or intradermal administration of Dp + nSP30, thus suggesting that the low IgG response

was a specific effect induced by cutaneous exposure to Dp + nSP30.

Effect of cutaneous exposure to Dp + nSP30 on susceptibility to anaphylaxis

Chemical mediators such as histamine and various cytokines induce the typical symptoms of atopic allergy, including inflammation and itching [30, 31]. The production of these chemical mediators is induced when an allergen cross-links IgE molecules bound to high-affinity IgE receptors (FcεRI) on mast cells and basophils. However, allergen-specific IgG, considered to be the 'blocking antibody', may neutralize allergen molecules before they can interact with IgE [32, 33]. Furthermore, IgG–allergen complexes act through a pathway regulated by the inhibitory receptor FcγRIIB to inhibit IgE-mediated mast cell and basophil signaling [32–34]. Therefore, the presence of allergen-specific IgG inhibits IgE-mediated allergic responses. Because our results showed that Dp + nSP30 led to low levels of Dp-specific IgG with little change in the levels of Dp-specific IgE (Fig. 3a–c), we examined whether this IgE-biased immune response induced by cutaneous exposure to Dp + nSP30 caused IgE-mediated hypersensitivity to Dp in a systemic anaphylaxis model. The decrease in rectal temperature after challenge with intravenous Dp was significantly greater in mice sensitized by Dp + nSP30 than in those sensitized by Dp alone (Fig. 4). That is, mice in the Dp + nSP30 group were more sensitive to the induction of Dp-specific anaphylaxis than were those in the Dp-alone group. Together, concurrent cutaneous exposure to Dp and nSP30 induced IgE-biased immune responses and, subsequently, increased sensitivity to anaphylaxis. In contrast, the functions of specific immunoglobulin subtypes vary between mice and humans; for example, blocking antibodies in humans are considered to be of the IgG4 subtype, which mice lack [35]. Therefore, our results cannot be extrapolated directly to humans. In addition, regulatory T and B cells have recently been suggested to be the main suppressors of atopic allergy in allergen-specific immunotherapy [36]. Additional study is needed to clarify whether increases in anaphylactic sensitivity is solely due to blocking antibody.

Effects of sequential cutaneous exposure to allergen and nSP30 on the IgE-biased immune response

We also evaluated the effects of sequential (rather than concurrent) cutaneous exposure to Dp and nSP30; that is, we topically applied Dp and nSP30 on alternate days rather than applying them together on the same day. Ear thickening and changes in total IgE concentration resulting from alternate-day application of Dp and nSP30 (Dp/nSP30) did not differ significantly from those resulting from concurrent treatment with Dp and PBS every other day (Dp/PBS) (Fig. 5a and b). Taken together, our results indicate that cutaneous exposure to nSP30 did not aggravate Dp-induced AD-like skin lesions regardless of whether the nanoparticles were applied together with or separately from Dp. In addition, alternate-day skin painting with Dp and nSP30 induced Dp-specific IgE and IgG production and Dp-specific IFN-γ- and IL-4-secreting splenocytes in the same way as did topical application of Dp and PBS (Fig. 5c–f). Therefore, exposure to both Dp and nSP30 was necessary to induce an IgE-biased immune response. Given that Dp + nSP30 formed agglomerates (Fig. 1), an interaction between Dp and nSP30 may have contributed to the subsequent IgE-biased immune response.

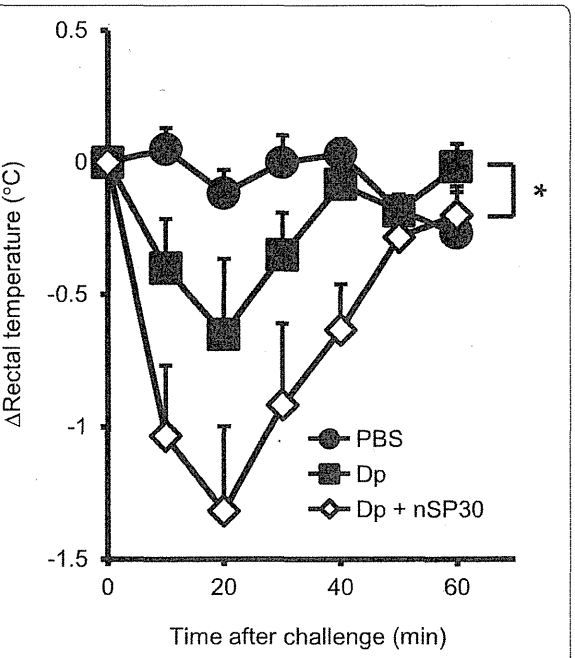

Fig. 4 Sensitivity to anaphylactic shock. Time-dependence of change in rectal temperature in NC/Nga mice due to intravenous challenge with Dp after treatment with Dp alone or Dp + nSP30 in PBS. Data are given as means ± SEMs ($n = 6$). *$P < 0.05$ vs. Dp-alone group

Effects of agglomeration of allergen and nSP30 on the IgE-biased immune response

Because the surface properties of nanomaterials strongly influence their interactions with proteins [37], we investigated how surface modification of nSP30 with carboxyl groups affected the interaction between Dp and nSP30 and the subsequent IgE-biased immune response. Solutions of the mixture of Dp and nSP30 modified with surface carboxyl groups (nSP30C) were clear and colorless (Fig. 1a), and a TEM image of Dp + nSP30C was similar to that of nSP30C alone (Fig. 1b). The mean hydrodynamic diameter of Dp + nSP30C was 24.8 nm, which